Int. J. Electrochem. Sci., 13 **(2018)** 10470 – 10479, doi:10.20964/2018.11.64

International Journal of
ELECTROCHEMICAL
SCIENCE
www.electrochemsci.org

Short Communication

Corrosion Behaviors of 5A06 Aluminum Alloy in Ethylene Glycol

Xiaoguang Zhang[1], *Xiang Liu*[2], *Wenping Dong*[2], *Gengkai Hu*[1], *Pan Yi*[3], *Yunhua Huang*[3], *Kui Xiao*[3,*]

[1] School of Aerospace Engineering, Beijing Institute of Technology, No.5 South Zhongguancun Street, Beijing 100081, China
[2] National key laboratory of human factors engineering, China astronaut research and training center, Beijing 100094, China
[3] Institute of Advanced Materials and Technology, University of Science and Technology Beijing, Beijing 100083, China
[*]E-mail: xiaokui@sina.com

Received: 19 June 2018 / *Accepted:* 20 August 2018 / *Published:* 1 October 2018

As a coolant, ethylene glycol solution can influence the corrosion processes of 5A06 aluminum alloys that are used for aerospace applications. The corrosion behavior of 5A06 in contact with pure ethylene glycol was investigated via 3D confocal laser scanning microscopy, scanning electron microscopy and electrochemical impedance spectroscopy. The results demonstrated that pure ethylene glycol may suppress the anodic dissolution of the aluminum alloy, thus decreasing the corrosion rate in pure ethylene glycol. Furthermore, the protective effect of oxidation films was enhanced as the result of a layer of Al-alcohol products that formed above the oxidation films in ethylene glycol.

Keywords: Aluminum alloy, corrosion mechanisms, ethylene glycol, organic, EIS

1. INTRODUCTION

Al-based alloys have been the primary material in the aerospace field for many years because of their excellent mechanical behavior [1]. In particular, 5A06 aluminum alloy has been applied in this field because of its low density, high elongation rate and high strength-to-weight ratio. Spacecraft generate a large amount of heat during launch and operation. Condensates such as ethylene glycol in the condensing system circulate in the pipes and serve as coolants. However, prolonged immersion in the coolants may cause corrosion problems with metal materials, which affects the safety of the spacecraft [2].

A few research studies have focused on the corrosion behaviors of aluminum in ethylene glycol solution. Chen [3] investigated the corrosion behaviors of 3003 aluminum alloy in an ethylene glycol solution that contained Cl^- at different temperatures, and the results demonstrated that the corrosion rate increased as the temperature rose. Niu [4] found that the anodic current density increased with an increase in temperature and that at 88℃, the aluminum alloy transformed from passive to active dissolution. In an aqueous environment, corrosive ions in ethylene glycol solution such as Cl^-, Cu^{2+} and Fe^{3+} led to accelerated corrosion of the aluminum alloy [5]. It was also found that the aluminum was inclined to erosion corrosion when ethylene glycol coolant was in the fluid state [6]. In contrast, ethylene glycol may provide a corrosion-inhibiting effect on aluminum alloys. For example, Zhang [7] found that a layer of Al-alcohol that suppressed the anodic dissolution formed above the native oxidation film at the ethylene glycol-water solution and aluminum alloy interface. Zaharieva [8] found that the presence of sebacic acid in ethylene glycol water solution had protective effects on aluminum alloys.

However, most of these studies focused on the effects of corrosive containment in ethylene glycol-water solutions, not pure ethylene glycol solution. In this study, the corrosion behaviors of AA 5A06 in both pure ethylene glycol and NaCl solution were investigated to better understand the difference between pure ethylene glycol and corrosive ions. 3D confocal laser scanning microscopy (3D LSCM) and environmental scanning electron microscopy (ESEM) were used to observe the pitting corrosion on aluminum alloy surfaces, and electrochemical impedance spectroscopy (EIS) was conducted to investigate the electrochemical behaviors of aluminum alloy surfaces.

2. EXPERIMENTAL METHODS

2.1 Materials prepared and corrosion text

Aluminum alloy 5A06 samples were cut and polished into dimensions of φ25 mm and φ15 mm. Samples of φ25 mm were etched individually in pure $(CH_2OH)_2$ solution and 3.5% (w.t.) NaCl solution for up to 10 days. The compositions (wt%) of 5A06 samples are as follows: 92.30% Al, 6.23% Mg, 0.73% Mn, 0.32% Fe, 0.99% Ti and 0.13% Others.

2.2 Morphologies analyses

A 3D confocal laser scanning microscope (3D CLSM, VK-X250) and an environmental scanning electron microscope (ESEM, FEI Quanta 250) were used to observe the surface morphology of samples after 10 days of immersion. The specimens with and without corrosion products were both characterized by 3D CLSM and SEM. The depths of the pits on the aluminum alloy were measured by 3D CLSM.

2.3 EIS test

A PARSTAT 2273 electrochemical workstation was used as an EIS measuring instrument. The electrochemical measurements were performed using a three-electrode cell. The 5A06 aluminum alloy samples of φ25 mm acted as the working electrode. A platinum foil was used as the counter electrode, and a saturated calomel electrode (SCE) was employed as the reference electrode. EIS measurement was conducted under the open-circuit potential in $(CH_2OH)_2$ electrolyte solution and 3.5% NaCl electrolyte solution separately with a scanning frequency from 100 kHz to 10 mHz and a disturbance potential of 10 mV. ZSimpWin software was used to fit the EIS data. The test times were 1, 3, 4 and 7 days.

3. RESULTS AND DISCUSSION

3.1 The morphologies of pitting corrosion

Samples immersed in 3.5% NaCl solution underwent more severe corrosion than samples immersed in $(CH_2OH)_2$ solution after 10 days (Figure 1). A large area of bluish green corrosion products covered the surfaces of the specimens that were immersed in 3.5% NaCl for up to 10 days (Figure 1a). After rust removal, a halo-shaped area caused by the deposition of Cl^- could be noticeably observed on the samples, illustrating that the samples etched in 3.5% NaCl solution suffered serious corrosion. No significant corrosion products could be observed on the samples (Figure 1b and c), which indicated that the $(CH_2OH)_2$ solution had no obvious corrosive effect on 5A06 Al-alloy samples during the 10 day immersion period.

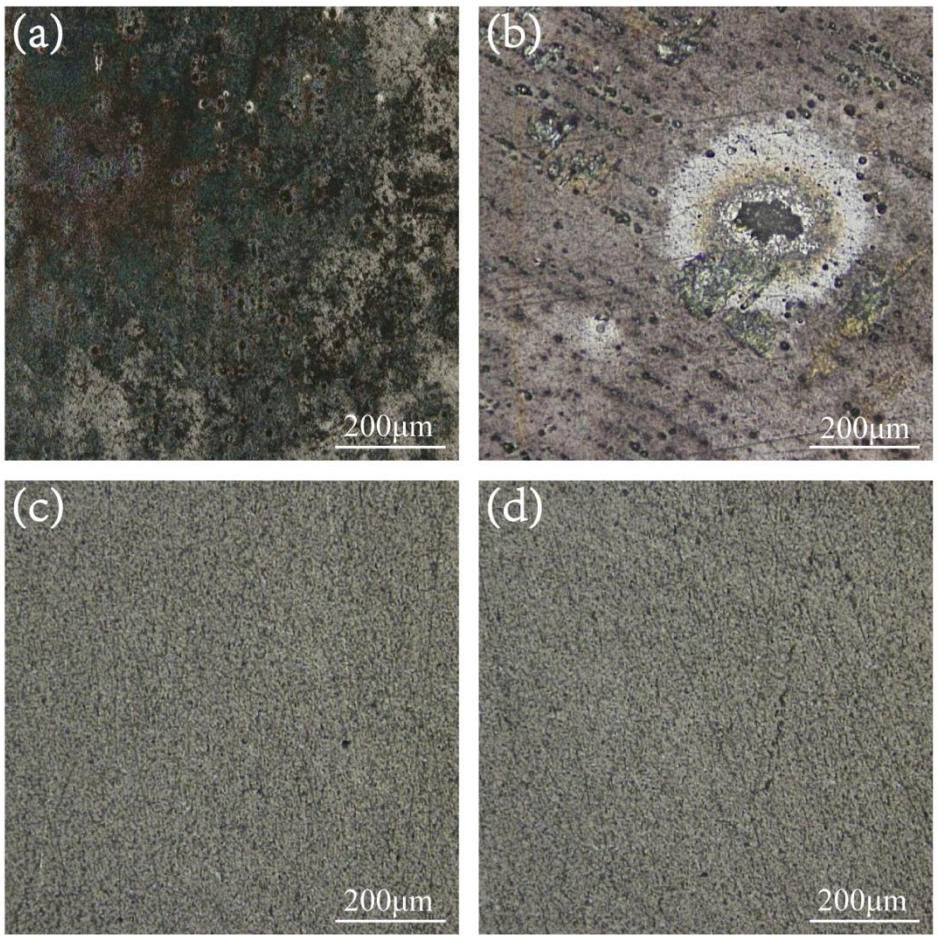

Figure 1. CLSM morphology of 5A06 specimens after 10 days of immersion: (a) in 3.5% NaCl solution without rust removal, (b) in 3.5% NaCl solution after rust removal, (c) in $(CH_2OH)_2$ solution without rust removal and (d) in $(CH_2OH)_2$ solution after rust removal.

The depths of pitting corrosion that occurred on samples immersed in 3.5% NaCl solution for up to 10 days were measured by 3D LSCM (in Figure 2b). The deepest pit had a depth of 21.628 μm. However, the surfaces of the sample immersed in $(CH_2OH)_2$ solution were much flatter than those immersed in NaCl solution (Figure 2 d). The maximum pit depths of the samples etched in 3.5% NaCl solution were deeper than those of samples etched in $(CH_2OH)_2$ solution, which indicated that the aluminum alloys that were immersed in $(CH_2OH)_2$ solution had excellent anti-corrosion properties.

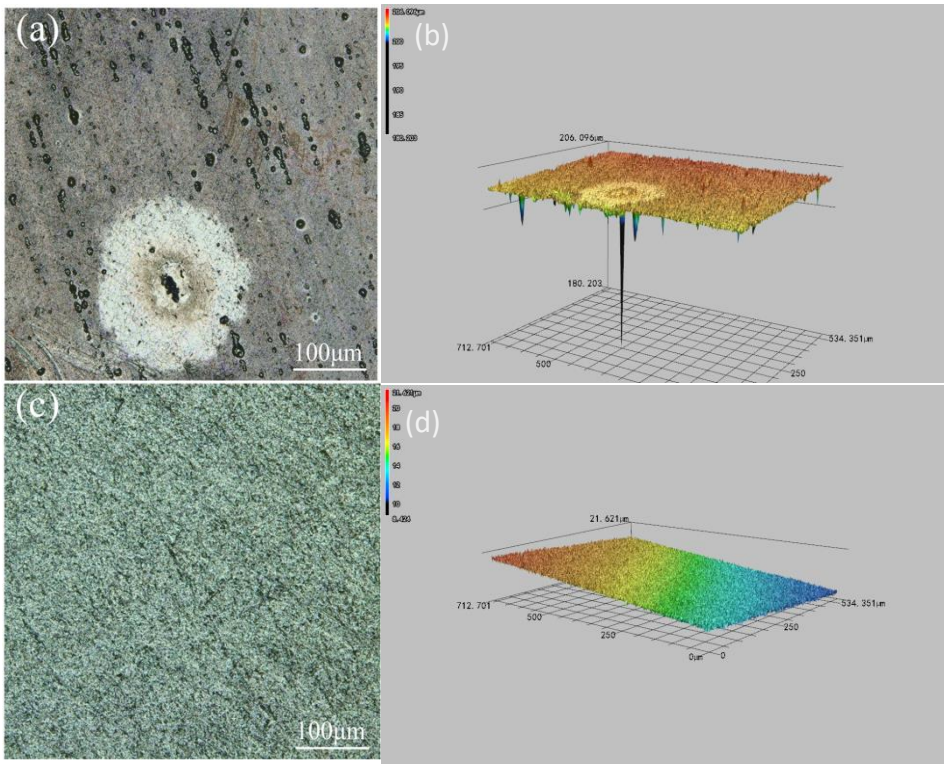

Figure 2. 3D morphology analysis and the depths of pits after 10 days of immersion. (a) CLSM morphology of 5A06 specimen in 3.5% NaCl solution after rust removal, (b) 3D morphology of the surface in Figure 2a; (c) CLSM morphology of 5A06 specimen in $(CH_2OH)_2$ solution and (d) 3D morphology of the surface in Figure 2c.

3.2 The SEM morphologies of aluminum alloy

SEM images of the samples etched in 3.5% NaCl solution and $(CH_2OH)_2$ solution after 10 days are shown in Figure 3. For the specimen soaked in NaCl solution, a few pits with different sizes and depths appeared scattered on the surface (Figure 3 (a) and (b)), which indicated that the aluminum alloy in NaCl solution suffered pitting corrosion. The light regions in the SEM images may be the secondary phases in the aluminum alloy, which were also observed in Leblanc's study [9].

However, after 10 days of immersion, the surface of the specimen soaked in $(CH_2OH)_2$ was extremely flat and remained intact, and there were just a few tiny pits that were defects on the aluminum surfaces evenly distributed on the surface, demonstrating that the specimens immersed in $(CH_2OH)_2$ did not suffer pitting corrosion. Because the aluminum alloy mainly underwent pitting corrosion at room temperature, the corrosive influence of $(CH_2OH)_2$ solution was much lower than that of Cl^-.

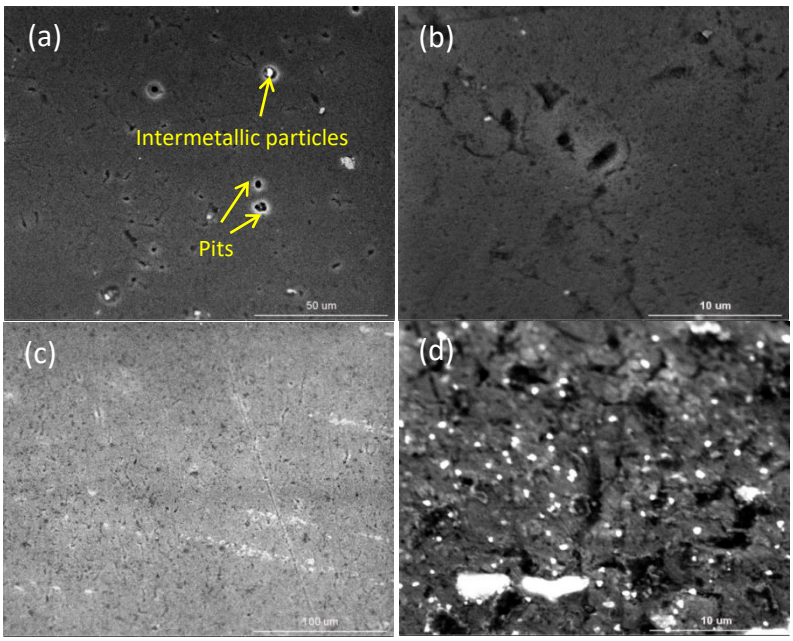

Figure 3. SEM images of the 5A06 specimens after 10 days of immersion with rust removal: (a) and (b) in 3.5% NaCl solution; (c) and (d) in $(CH_2OH)_2$ solution.

3.3 EIS study of aluminum alloy

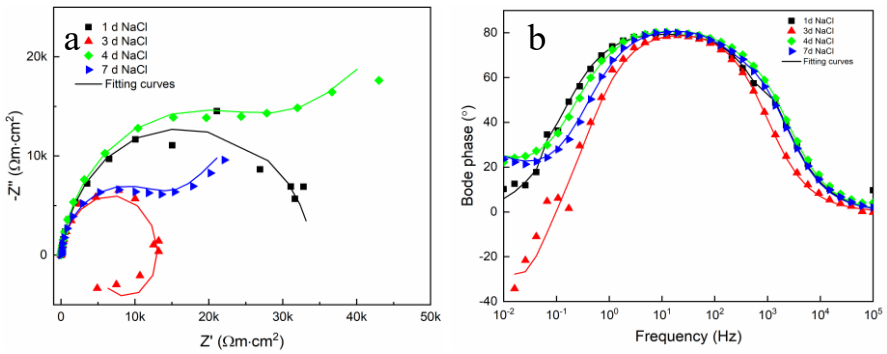

Figure 4. The Nyquist diagrams and Bode plots of specimens that were immersed in 3.5% NaCl solution for different exposure times: (a) Nyquist and (b) Bode plots.

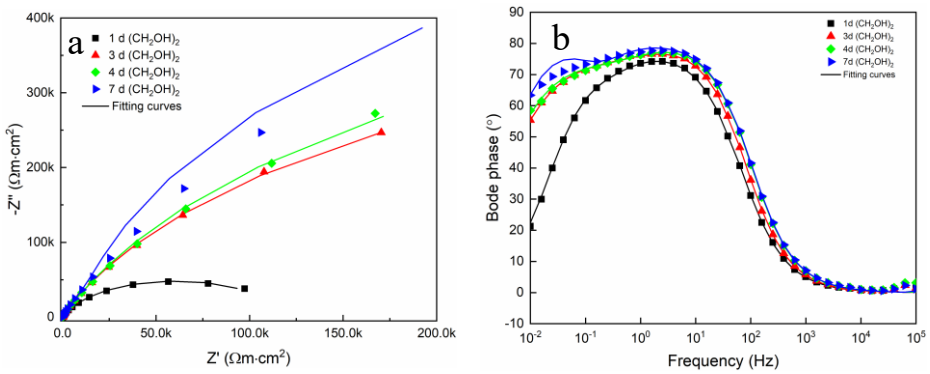

Figure 5. The Nyquist diagrams and Bode plots of specimens that were immersed in $(CH_2OH)_2$ solution for different exposure times: (a) Nyquist and (b) Bode plots.

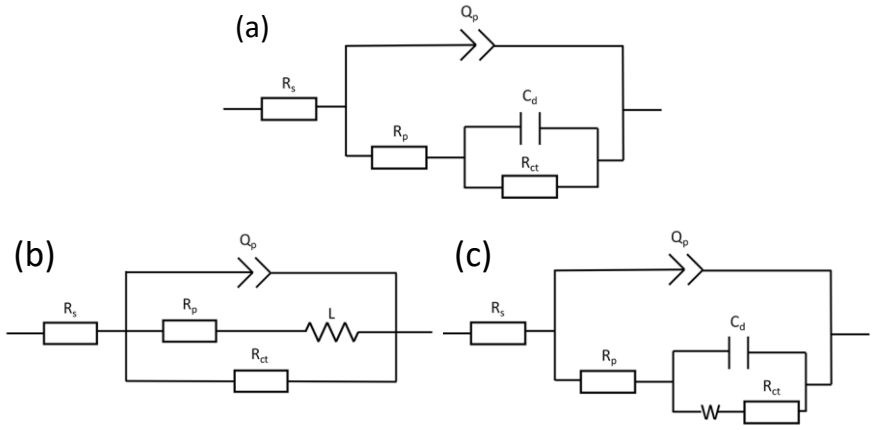

Figure 6. The equivalent circuits for EIS of specimens that were immersed in 3.5% NaCl solution for different exposure times: (a) 1 d, (b) 3 d, (c) 4 d and 7 d.

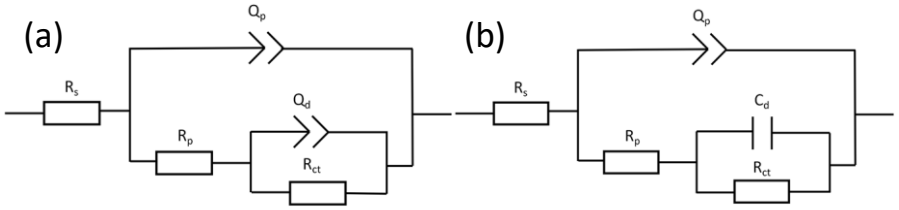

Figure 7. The equivalent circuits for EIS of specimens that were immersed in $(CH_2OH)_2$ solution for different exposure times: (a) 1 d, 3 d, 4 d, and (b) 7 d.

Table 1. The fitting results of EIS for specimens that were immersed in 3.5% NaCl solution for different exposure days.

Times (d)	R_s ($\Omega\cdot cm^2$)	Q_p ($\mu F\cdot cm^{-2}\cdot S^{-n-1}$)	n	R_p ($k\Omega\cdot cm^2$)	C_d ($\mu F\cdot cm^{-2}$)	R_{ct} ($k\Omega\cdot cm^2$)	W ($\Omega^{-1}\cdot cm^{-2}\cdot S^{-1/2}$)	L ($\mu H\cdot cm^2$)
1	6.701	29.09	0.901	28.69	471.2	5.370	-	
3	12.55	26.79	0.913	6.980		13.82	-	934.3
4	6.023	26.25	0.912	0.373	1.657	27.31	1.762×10^{-4}	
7	5.279	31.95	0.919	0.216	3.300	13.19	3.168×10^{-4}	

Table 2. The fitting results of EIS for specimens that were immersed in $(CH_2OH)_2$ solution for different exposure days.

Times (d)	R_s ($\Omega\cdot cm^2$)	Q_d ($\mu F\cdot cm^{-2}\cdot S^{-n1-1}$)	n_1	R_p ($k\Omega\cdot cm^2$)	C_p or Q_p ($\mu F\cdot cm^{-2}\cdot S^{-n2-1}$)	n_2	R_{ct} ($k\Omega\cdot cm^2$)
1	1032	37.96	0.879	53.54	19.35	0.864	65.60
3	118.4	23.42	0.903	51.04	7.226	0.672	882.1
4	99.65	22.51	0.904	57.99	7.543	0.697	1014
7	103.7	21.39	0.903	174.8	7.091	-	1174

There are two constants in the equivalent circuits for the aluminum alloy both in NaCl solution and $(CH_2OH)_2$ solution (in Figure 6 and 7, respectively). In general, the constant located in the high frequency region represents the oxidation films of the aluminum alloy, and the constant located in the low frequency region reflects the charge transfer step in the corrosion processes [10, 11].

For specimens soaked in NaCl solution, after immersion for 3 days, an inductance arc formed in the low frequency region (in Figure 4a), which indicated that the protective effect of oxidation films of aluminum had been suppressed because of the Cl^-. After 4 days of exposure, the inductance disappeared and a Warburg resistance occurred in the low frequency region (in Figure 4a), which indicated that the diffusion step had been the dominant step of all the electrochemical reactions [12], and the aluminum alloy had entered the pitting development stage. From 3 to 4 days, the value of R_p decreased significantly, from 6.980 $k\Omega \cdot cm^2$ to 0.373 $k\Omega \cdot cm^2$ (Table 1), meaning that the protective effect of the oxidation films had vanished and pitting corrosion had penetrated into the aluminum substrate. Typically, the value of R_{ct} is inversely proportional to corrosion rate [13, 14]. With the prolonged immersion in Cl^- aqueous, the value of R_{ct} decreased, which demonstrated that the corrosion process accelerated (Table 1).

For specimens soaked in $(CH_2OH)_2$ solution, there was an increase in the value of R_p (Table 2), indicating that the protective effect of the oxidation films had been enhanced. The value of R_{ct} rose constantly with prolonged soaking in $(CH_2OH)_2$ solution (Table 2), which indicated that the $(CH_2OH)_2$ solution had an inhibition effect on the aluminum alloy.

3.4 The corrosion mechanisms

The aluminum alloy instantaneously generates a layer of oxidation films that consists of Al_2O_3, AlO(OH), and $Al(OH)_3$ on the surface of the aluminum alloy when the alloy substrate contacts the air or solution [15]. The good anti-corrosion properties of aluminum alloys mainly comes from this oxidation film [16]. However, the protective effect of oxidation films can be reduced by the Cl^- that exists in solution.

When the aluminum specimens were soaked in NaCl solution, Cl^- ions adsorbed at the oxidation film defect sites, and an inductance arc appeared after 3 days of immersion. Kedam [17] argued that the presence of the inductance arc indicated the weakness of oxidation films. Owing to the heterogeneity of secondary phases in aluminum alloy, the oxidation films on these area were prone to the adsorption of Cl^-. When Cl^- adsorbed, the insoluble $Al(OH)_3$ gradually generated water-soluble $AlCl_3$ in the oxidation films [18]. Thus, the productive effect was rapidly reduced in these defect regions. Therefore, the value of R_p declined obviously. After 4 days, the pitting corrosion occurred at local regions where the oxidation films had been dissolved, and pits occurred on the substrates of the aluminum alloy. Hence, in the low frequency region, a Warburg resistance represented the inductance arc. With the development of pitting corrosion, the corrosion rate was accelerated [19]. Thus, a decrease in the value of R_{ct} appeared after 4 days. The corrosion processes are as follows [15]:

Anodic:

$$Al \rightarrow Al^{3+} + 3e^{-} \quad (1)$$

Cathodic:

$$O_2 + 2H_2O + 4e^{-} \rightarrow 4OH^{-} \quad (2)$$

After 10 days of immersion in NaCl solution, the morphologies of pitting corrosion that were pit on the surfaces of the aluminum alloy were observed in 3D CLSM and SEM. On the initial corrosion of aluminum alloy, a type of morphology called "circumferential" pits appeared as a ring around secondary phases and sometimes the intermetallic particles remained in the pits [20]. After 10 days of exposure to NaCl solution, the pits were mainly distributed around the secondary phases and the intermetallic particles that were light regions in SEM could be observed inside the pits (Figure 3a). The depths of pits were detected by 3D CLSM (Figure 2b). However, in $(CH_2OH)_2$ solution, the electrochemical reactions were as follows [3]:

Anodic:

$$Al \rightarrow Al^{3+} + 3e^{-}$$

$$Al^{3+} + 3(HO - CH_2CH_2 - O^{-}) \rightarrow Al(HOCH2CH2O)_3 \quad (3)$$

Cathodic:

$$O_2 + 2H_2O + 4e^{-} \rightarrow 4OH^{-} \quad (4)$$

Similarly, in Zhang's study [7], a layer of Al-alcohol products that suppressed the anodic dissolution could form in ethylene glycol water solution. Thus, the products of $Al(HOCH_2CH_2O)_3$ had an inhibition effect on the aluminum alloy corrosion processes. In addition to $Al(HOCH_2CH_2O)_3$, some organic compounds that contained (-OH) contributed to the self- repair performance of oxidation films. Ornek [21] found that in the secretions of some bacteria, organic compounds that consisted of (-OH) could restrain the dissolution of aluminum oxidation films and result in the inhibition of pitting corrosion.

Therefore, in pure $(CH_2OH)_2$ solution that had no Cl^-, the protective effect of the oxidation films could be reinforced, resulting in an increase in the value of R_p. Simultaneously, the corrosion rate was reduced as a result of the inhibition of anodic reaction. Consequently, the value of *Rct* increased continuously. In brief, the inclination of pitting corrosion of aluminum in pure $(CH_2OH)_2$ solution was much lower than that in a solution containing Cl^-. Hence, the 3D and SEM morphologies of surfaces in $(CH_2OH)_2$ solution had no sign of pitting corrosion.

4. CONCLUSIONS

In 3.5% NaCl solution, corrosion was accelerated because of Cl^-, and pitting corrosion occurred on the 5A06 aluminum after 3 days of immersion. However, in pure $(CH_2OH)_2$ solution, a layer of Al-alcohol products formed above the oxidation films of 5A06 aluminum alloy, which contributed to the protective effect of the oxidation films. The Al-alcohol layer could inhibit the anodic dissolution of 5A06 aluminum alloy and reduce the corrosion rate, thereby resulting in a decrease in R_p and R_{ct}. After

10 days of immersion in pure $(CH_2OH)_2$ solution, the surfaces of the aluminum alloy still remained intact, and no obvious sign of pitting corrosion was observed by 3D CLSM and SEM.

ACKNOWLEDGEMENTS
This work was supported by the National Basic Research Program of China (973 Program, No. 2014CB643300), and the National Environment Corrosion Platform (NECP).

References

1. X. Zhang, Y. Chen and J. Hu, *Prog. Aerosp. Sci.*, 97 (2018) 22.
2. G. Song and D. Stjohn, *Corros. Sci.*, 46 (2004) 1381.
3. X. Chen, W. Tian and S. Li, *Chinese J. Aeronaut.*, 29 (2016) 1142.
4. L. Niu and Y.F. Cheng, *Wear*, 265 (2008) 367.
5. O.K. Abiola, and J.O.E.Otaigbe, *Corros. Sci.*, 50 (2008) 242.
6. G.A. Zhang, L.Y. Xu and Y.F. Cheng, *Corros. Sci.*, 51 (2009) 283.
7. G.A. Zhang, L.Y. Xu and Y.F. Cheng, *Electrochim. Acta*, 53 (2008) 8245.
8. J. Zaharieva, M. Milanova and M. Mitov, *J. Alloy. Compd.*, 470 (2009) 397.
9. P. Leblanc P and G.S. Frankel, J. *Electrochem. Soc.*, 149 (2002) B239.
10. Z. Cui, X. Li and H. Zhang, *Adv. Mate. Sci. Eng*., 2015 (2015) 1.
11. Z. Bai, K. Xiaon and L. Chen, Int. *J. Electrochem. Sc.*, 13 (2018) 2033
12. P. Yi, K. Xiao and K. Ding, *Mater. Res. Bull.*, 91 (2017) 179.
13. K. Xiao, Z. Bai and L. Yan, *J. Mater. Sci - Mater. El.*, 29 (2018) 8877.
14. K. Xiao, X. Gao and L. Yan, *Chem. Eng. J.*, 339 (2017) 92.
15. T. Li, X.G. Li and C.F. Dong, *J. Mater. Eng. Perform.*, 19 (2010) 591 .
16. Y. Liu and Y.F. Cheng, *J. Appl. Electrochem.*, 39 (2009) 1267.
17. M. Keddam, C.Kuntz and H. Takenouti, *Electrochim. Acta*, 42 (1997) 87.
18. Z.Y. Cui, X.G. Li, and K. Xiao, Corros. *Eng. Sci. Techn.*, 50 (2015) 438.
19. L. Lei, X. Li and C. Dong, *Electrochim. Acta*, 54 (2009) 6389.
20. N. Birbilis and R.G. Buchheit, *J. Electrochem. Soc.*, 155 (2008) 3293.
21. D. Ornek, A. Jayaraman and B.C. Syrett, *Appl. Microbiol. Biotechnol.*, 58 (2002) 651.